

This is a repository copy of *Gas-phase structures of sterically crowded disilanes studied by electron diffraction and quantum chemical methods: 1,1,2,2-tetrakis(trimethylsilyl) disilane and 1,1,2,2-tetrakis(trimethylsilyl)dimethyldisilane*.

White Rose Research Online URL for this paper:

<https://eprints.whiterose.ac.uk/id/eprint/93803/>

Version: Accepted Version

Article:

Schwabedissen, Jan, Lane, Paul D., Masters, Sarah L. et al. (2 more authors) (2014) Gas-phase structures of sterically crowded disilanes studied by electron diffraction and quantum chemical methods: 1,1,2,2-tetrakis(trimethylsilyl) disilane and 1,1,2,2-tetrakis(trimethylsilyl)dimethyldisilane. Dalton Transactions. pp. 10175-10182. ISSN: 1477-9226

<https://doi.org/10.1039/c4dt00628c>

Reuse

Items deposited in White Rose Research Online are protected by copyright, with all rights reserved unless indicated otherwise. They may be downloaded and/or printed for private study, or other acts as permitted by national copyright laws. The publisher or other rights holders may allow further reproduction and re-use of the full text version. This is indicated by the licence information on the White Rose Research Online record for the item.

Takedown

If you consider content in White Rose Research Online to be in breach of UK law, please notify us by emailing eprints@whiterose.ac.uk including the URL of the record and the reason for the withdrawal request.

Gas-phase structures of sterically crowded disilanes studied by electron diffraction and quantum chemical methods: 1,1,2,2-tetrakis(trimethylsilyl)disilane and 1,1,2,2-tetrakis(trimethylsilyl)dimethyldisilane †‡

Jan Schwabedissen,^a Paul D. Lane,^b Sarah L. Masters,^{*,c} Karl Hassler^d and Derek A. Wann^{*,b}

^a *Fakultät für Chemie, Anorganische Chemie und Strukturchemie, Universitätsstr. 25, 33615 Bielefeld, Germany.*

^b *Department of Chemistry, University of York, Heslington, York, U.K. YO10 5DD. E-mail: derek.wann@york.ac.uk*

^c *Department of Chemistry, University of Canterbury, Private Bag 4800, Christchurch 8140, New Zealand. E-mail: sarah.masters@canterbury.ac.nz*

^d *Technische Universität Graz, Stremayergasse 16, A-8010 Graz, Austria.*

Abstract

The gas-phase structures of the disilanes 1,1,2,2-tetrakis(trimethylsilyl)disilane [(Me₃Si)₂HSiSiH(SiMe₃)₂] (**1**) and 1,1,2,2-tetrakis(trimethylsilyl)dimethyldisilane [(Me₃Si)₂MeSiSiMe(SiMe₃)₂] (**2**) have been determined by density functional theoretical calculations and by gas electron diffraction (GED) employing the SARACEN method. For each of **1** and **2** DFT calculations revealed four C₂-symmetric conformers occupying minima on the respective potential-energy surfaces; three conformers were estimated to be present in sufficient quantities to be taken into account when fitting the GED data. For (Me₃Si)₂RSiSiR(SiMe₃)₂ [R = H (**1**), CH₃ (**2**)] the lowest energy conformers were found by GED to have RSiSiR dihedral angles of 87.7(17)° for **1** and -47.0(6)° for **2**. For each of **1** and **2** the presence of bulky and flexible trimethylsilyl groups dictates many aspects of the geometric structures in the gas phase, with the molecules often adopting structures that reduce steric strain.

[†] This article is published in celebration of the 50th anniversary of the opening of the Chemistry Department at the University of York.

[‡] Electronic supplementary information (ESI) available: additional details relating to the GED experiments (Table S1); least-squares correlation matrices (Tables S2 and S3); calculated coordinates and energies (Tables S4-S7); descriptions of the models used for the refinements, refined (r_{hl}) and calculated (r_{e}) parameters values and their SARACEN restraints used in the three-conformer least-squares refinements of **1** and **2** (Tables S8 and S9), amplitudes of vibration and curvilinear distance corrections (Tables S10 and S11); final GED coordinates (Tables S12 and S13); plots of the amount of conformer against $R_{\text{G}}/R_{\text{G}}(\text{min.})$ (Figure S1); plots of molecular-scattering intensity curves (Figure S2).

Introduction

The structures of disilanes, functionalised derivatives of Si_2H_6 , have received much attention because of their wide-ranging uses in chemistry and materials science.¹ For example, disilanes form the backbones of polymers, while some of their monomeric moieties are used to stabilise compounds containing elements in low oxidation states.² Furthermore, the rotational isomerism exhibited by disilanes in the gas phase is a feature that has been extensively studied using both experimental (gas electron diffraction and Raman spectroscopy) and computational methods.

In recent decades the structures of a number of disilane derivatives have been investigated using gas electron diffraction complemented by computational methods. For homoleptic disilanes general trends in the Si–Si bond lengths have been attributed on the basis of the electron-withdrawing and electron-donating character of the substituents attached to the silicon atoms. Using disilane, Si_2H_6 ,³ as a reference the Si–Si bond is observed to shorten upon inclusion of electronegative halogen atoms to give Si_2F_6 ⁴ and Si_2Cl_6 ,⁵ while the bond is lengthened by the inclusion of electron-donating methyl groups in Si_2Me_6 .⁶ The structures of these, as well as of the partially halogenated disilanes 1,1,2,2-tetrabromodisilane,⁷ 1,2-diiododisilane,⁸ and 1,1,2,2-tetraiododisilane,⁸ show the expected staggered conformations in the gas phase.

Further work has been performed to substitute disilanes with more sterically-demanding groups such as *tert*-butyl, leading to some surprising structures in the gas phase. While disilanes with two *tert*-butyl groups (1,2-di-*tert*-butyldisilane⁹ and 1,2-di-*tert*-butyltetrafluorodisilane¹⁰) prefer to exist in *anticlinal* conformations, the increasingly sterically-crowded 1,1,2-tri-*tert*-butyldisilane¹¹ has an almost eclipsed arrangement, with each *tert*-butyl group eclipsing a hydrogen atom to minimise interactions with other *tert*-butyl groups.

In 1,1,2,2-tetra-*tert*-butyldisilane¹² the steric crowding results in the preferred conformer being an ortho¹³ (*anticlinal*) conformer. This structure has an HSiSiH dihedral angle of $94.2(18)^\circ$,¹³ in which two *tert*-butyl groups are eclipsing hydrogen atoms attached to the other silicon atom. The elongation of the Si–Si bond to 245.2(8) pm [from 233.1(3) pm as observed for Si_2H_6 ³] is due to the electron-donating character of the substituents, as well as to the steric effects of the *tert*-butyl groups.

Hexa-*tert*-butyldisilane,¹⁴ in which the central Si–Si core has been fully substituted with *tert*-butyl groups and is known as superdisilane, has also been studied. In the crystalline phase it has an Si–Si bond length of 269.7(3) pm, which cannot be compared experimentally with its gas-phase equivalent because superdisilane decomposes into “half-dimer” radicals.¹⁵

A natural progression from studying the effects on geometry of *tert*-butyl groups is to switch to using trimethylsilyl groups, as has been done for (Me₃Si)₂HSiSiH(SiMe₃)₂ (**1**) and (Me₃Si)₂MeSiSiMe(SiMe₃)₂ (**2**) which are studied using gas electron diffraction and computational methods in this work. Substituting the central carbon atom in a *tert*-butyl group for a silicon atom will result in longer bonds to the bulky groups, and should allow for more flexibility in the geometries of the substituents. Furthermore, the abilities of the hydrogen atom and methyl group substituents (in **1** and **2**, respectively) to compensate for the steric crowding and strain can be deduced from the gas-phase structures.

Experimental

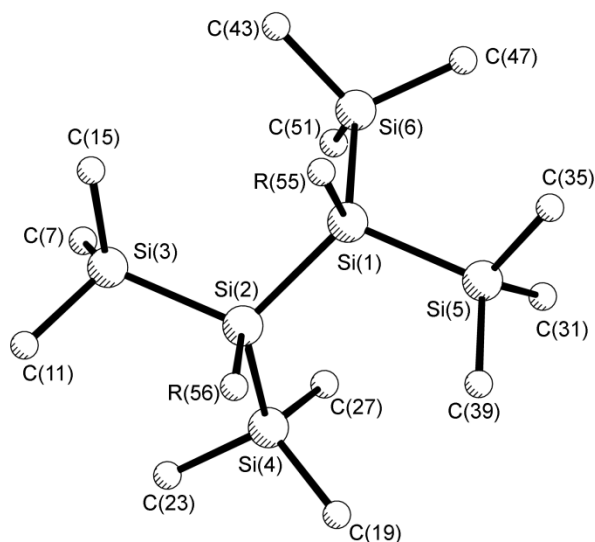
Syntheses of (Me₃Si)₂HSiSiH(SiMe₃)₂ and (Me₃Si)₂MeSiSiMe(SiMe₃)₂

Samples of both **1** and **2** were prepared according to the literature methods.^{16,17} The samples were purified either by distillation (**1**) to give an oil, or by sublimation (**2**) to give a white solid. Both samples were examined by NMR spectroscopy to verify their purities. The samples were subsequently used for the GED experiments without further purification.

Computational methods

Previous work on similar disilane systems showed that there are often several minima on the potential-energy surface. This gives rise to conformers that are linked through rotation of the central Si–Si bond. See Figure 1 for a diagrammatic representation of one conformer of **1** (R = H) or **2** (R = CH₃).

Figure 1 The molecular geometry of a low-energy conformer of $(\text{Me}_3\text{Si})_2\text{RSiSiR}(\text{SiMe}_3)_2$ [$\text{R} = \text{H}$ (**1**), CH_3 (**2**)] showing atom numbering for the major conformers **1a** and **2a**. Hydrogen atoms have been removed for clarity. For **1** the numbering of conformers **1b** and **1c** is obtained by adding 56 and 112, respectively, to the numbering of **1a**, while for **2b** and **2c** 62 and 124 must be added to the numbering of **2a**, respectively.



To identify all possible minima that exist for **1** and **2**, initial potential-energy surface scans were performed by rotating about the Si(1)–Si(2) bonds. These scans were carried out at the Hartree-Fock level using the 6-31G(d) basis set on all atoms.

All calculations performed in the course of this work used the Gaussian 09 suite of programs¹⁸ running on either the University of Edinburgh’s ECDF cluster,¹⁹ or on the U.K. National Service for Computational Chemistry Software clusters.²⁰ Once potential minima had been identified, geometry optimisations and frequency calculations were carried out to determine the energetics of any minimum-energy conformers. The B3LYP method^{21–23} with a 6-311G(2d,p)^{24,25} basis set were used for these calculations. Further geometry optimisations and frequency calculations were carried out on conformers deemed to have sufficiently low energies. As a comparison, geometry optimisations were performed for each conformer using the B3LYP augmented with Grimme’s dispersion method²⁶ (B3LYP-GD3) again with the 6-311G(2d,p) basis set.

For a given species, the relative abundance (N_i) of conformer i that is likely to exist in the gas phase at the temperature (T) of the GED experiment was estimated using Equation (1), the Boltzmann distribution:

$$\frac{N_i}{\sum_i N_i} = \frac{g_i \exp(-\Delta G_i / RT)}{\sum_i g_i \exp(-\Delta G_i / RT)}, \quad (1)$$

where (ΔG_i) is the Gibbs free energy of conformer i as determined by quantum chemical calculations, g_i is the statistical weight for that conformer, and R is the gas constant.

Gas electron diffraction (GED)

Data for **1** and **2** were collected using the GED apparatus that was housed in Edinburgh until 2010.²⁷ An accelerating potential of 40 keV was applied, producing electrons with an approximate wavelength of 6.0 pm. Experiments were performed for each disilane at two different nozzle-to-camera distances, increasing the range of angles through which data were collected. Accurate nozzle-to-camera distances were determined by analysing the results of diffraction experiments using gaseous benzene that were carried out immediately after collecting data for **1** and **2**. The scattering intensities were recorded on Kodak Electron Image films, and digitised using an Epson Expression 1680 Pro flat-bed scanner and converted to mean optical densities using a method described elsewhere.²⁸ A full list of experimental parameters can be found in Table S1.

The data were analysed using the ed@ed least-squares refinement program v3.0,²⁹ incorporating the scattering factors of Ross *et al.*³⁰ Weightings for the off-diagonal weight matrices, and scale factors can be found in Table S1, while Tables S2 and S3 show the correlation matrices.

Results

Calculated structures

Several minima were observed from the potential-energy surface scan for **1**, and geometry optimisations started from these structures yielded four unique conformers. The zero-point-corrected energies for these conformers were obtained by performing calculation at the B3LYP level with 6-311G(2d,p) basis set and, for comparison, using the B3LYP-GD3 method with the same basis set. The B3LYP-GD3 optimisations were started from the optimised B3LYP geometries. The relative free energies for each conformer for both calculations is given in Table 1, along with the HSiSiH dihedral angles that defines each conformer. From these calculations conformer **1d** has such a low predicted relative

abundance that it will not be included in the GED refinements. Table 2 shows selected geometric parameters for the three conformers included in the GED refinement.

Table 1 HSiSiH dihedral angle, symmetry, relative energy, and percentage abundance for each conformer of **1**.^a

Conformer	HSiSiH ^b	Assignment	Point-group symmetry	Relative energy ^c	Percentage abundance ^d
1a	90.1 / 87.1	<i>anticlinal</i>	C_2	0.0 / 0.0	78.2 / 50.9
1b	−98.1 / −120.7	<i>anticlinal</i>	C_2	+6.0 / +1.3	14.9 / 35.2
1c	−57.4 / −49.5	<i>synclinal</i>	C_2	+9.1 / +5.5	6.2 / 10.4
1d	−157.0 / −163.5	<i>antiperiplanar</i>	C_2	+17.5 / +9.3	0.7 / 3.5

^a Calculations performed using B3LYP/6-311G(2d,p) and B3LYP-GD3/6-311G(2d,p).

Values given for both calculations in that order. ^b These are the values of the H(56)Si(2)Si(1)H(55) dihedral angles in degrees; no interconversion was observed upon optimisation. See Figure 1 for atom numbering. ^c Gibbs free energy in kJ mol^{−1} (ZPE corrected). ^d Calculated using the Boltzmann equation using the average temperature of the GED experiment.

Table 2 Selected geometric parameters for **1a–1c**.^a

Parameter	GED			B3LYP/6-311G(2d,p)			B3LYP-GD3/6-311G(2d,p)		
	1a	1b	1c	1a	1b	1c	1a	1b	1c
<i>r</i> Si(1)Si(2)	237.4(1)	237.6(1)	237.4(1)	239.0	238.8	238.6	237.4	237.6	237.4
<i>r</i> Si(1)Si(5)	236.4(1)	236.1(1)	236.4(1)	238.0	237.9	238.5	236.8	236.5	236.8
<i>r</i> Si(1)Si(6)	236.6(1)	236.3(1)	237.2(1)	238.2	238.1	238.3	236.8	236.5	237.4
<i>r</i> Si(1)H(55)	150.2(16)	150.1(16)	150.1(16)	149.9	149.8	149.8	149.8	149.7	149.7
∠Si(5)Si(1)Si(6)	113.5(7)	111.9(7)	111.6(7)	114.8	112.7	112.4	112.5	111.0	110.7
∠Si(2)Si(1)Si(5)	117.1(4)	107.4(4)	112.3(4)	117.6	109.1	113.1	116.3	106.6	111.5
∠Si(2)Si(1)Si(6)	110.6(7)	121.1(7)	118.1(7)	110.2	120.3	118.5	108.9	119.4	116.4
∠Si(2)Si(1)H(55)	106.0(6)	106.0(6)	105.0(6)	104.8	104.4	102.8	106.1	106.1	105.1
∠H(55)Si(1)Si(5)	103.9(10)	105.8(10)	105.0(10)	103.6	105.0	102.8	105.7	107.6	106.8
∠H(55)Si(1)Si(6)	104.3(10)	103.4(10)	103.3(10)	104.2	103.6	103.9	106.5	105.6	105.5
∠Si(1)Si(5)C(31)	112.4(4)	108.8(4)	109.5(4)	110.8	110.6	111.6	112.2	108.8	109.3
∠Si(1)Si(6)C(51)	110.2(4)	110.6(4)	112.3(4)	111.6	112.0	112.7	110.0	110.4	112.1
ϕH(56)Si(2)Si(1)H(55)	87.7(17)	−102.0(44)	−52.0(41)	90.1	−98.1	−57.4	87.1	−120.7	−49.5

^a See Figure 1 for atom numbering. Distances (*r*) are in pm, angles (∠) and dihedral angles (ϕ) are in degrees. Values in parentheses are the uncertainties quoted as 1σ values.

The potential-energy scan performed by rotating about the Si(1)–Si(2) bond for **2** revealed eight possible conformers. Geometry optimisation performed using B3LYP/6-311G(2d,p), and subsequently using B3LYP-GD3/6-311G(2d,p) gave four unique conformers, with the other four minima representing enantiomeric forms of these. Frequency calculations were undertaken using the same level of theory and basis set, and the energies used to estimate the composition of **2** in the gas phase at the temperature of the GED experiment. As can be seen from Table 3, the calculated energies for conformer **2d** were significantly higher than for **2a–2c**, and so it was not taken into account in the determination of the GED structure. Table 4 shows selected geometric parameters for the three conformers included in the GED refinement.

Table 3 CSiSiC dihedral angle, symmetry, relative energy, and percentage abundance for each conformer of **2**.^a

Conformer	CSiSiC ^b	Assignment	Point-group symmetry	Relative energy ^c	Percentage abundance ^d
2a	−45.6 / −46.4	<i>synclinal</i>	<i>C</i> ₂	0.0 / 0.0	62.0 / 50.6
2b	−82.6 / −82.6	<i>synclinal</i>	<i>C</i> ₂	+3.8 / +1.7	22.0 / 30.8
2c	−159.6 / −161.7	<i>antiperiplanar</i>	<i>C</i> ₂	+5.9 / +4.7	12.4 / 13.1
2d	−129.4 / −138.8	<i>anticlinal</i>	<i>C</i> ₂	+10.4 / +7.8	3.6 / 5.5

^a Calculations performed using B3LYP/6-311G(2d,p) and B3LYP-GD3/6-311G(2d,p).

Values given for both calculations in that order. ^b These are the values for the C(56)Si(2)Si(1)C(55) dihedral angles in degrees. See Figure 1 for atom numbering. ^c Gibbs free energy in kJ mol^{−1} (ZPE corrected). ^d Calculated using the Boltzmann equation using the average temperature of the GED experiment.

Table 4 Selected geometric parameters for **2a–2c**.^a

Parameter	GED			B3LYP/6-311G(2d,p)			B3LYP-GD3/6-311G(2d,p)		
	2a	2b	2c	2a	2b	2c	2a	2b	2c
<i>r</i> Si(1)Si(2)	236.8(1)	237.0(1)	236.7(1)	240.1	240.6	240.2	237.7	237.9	237.6
<i>r</i> Si(1)Si(5)	236.2(1)	236.5(1)	237.2(1)	239.1	239.3	240.1	237.0	237.3	238.0
<i>r</i> Si(1)Si(6)	236.5(1)	236.2(1)	236.8(1)	239.1	238.9	239.4	237.3	237.0	237.6
<i>r</i> Si(1)C(55)	193.3(18)	193.4(18)	192.9(18)	192.1	192.2	191.8	191.7	191.8	191.3
∠Si(5)Si(1)Si(6)	109.3(11)	110.1(11)	108.7(12)	109.8	110.9	105.6	108.9	109.7	105.2
∠Si(2)Si(1)Si(5)	113.4(8)	112.0(8)	113.7(8)	112.7	111.0	112.1	111.2	109.7	111.4
∠Si(2)Si(1)Si(6)	117.9(4)	117.3(4)	114.8(4)	116.5	116.1	115.4	116.2	115.6	113.1
∠Si(2)Si(1)C(55)	103.8(6)	106.3(6)	106.5(6)	106.0	108.4	108.8	106.2	108.7	108.9
∠C(55)Si(1)Si(5)	106.2(7)	105.2(7)	109.2(7)	104.8	104.3	108.5	106.8	105.8	109.8
∠C(55)Si(1)Si(6)	107.0(2)	106.9(2)	108.4(2)	106.1	105.4	106.2	107.0	106.9	108.4
∠Si(1)Si(5)C(31)	111.7(8)	113.6(8)	110.9(8)	112.6	113.8	111.1	110.7	112.6	109.9
∠Si(1)Si(6)C(51)	113.5(4)	111.8(4)	111.2(4)	113.4	113.0	112.6	113.1	111.4	110.8
ϕC(56)Si(2)Si(1)C(55)	−47.0(6)	−73.3(26)	−161.9(16)	−45.9	−82.6	−159.6	−46.4	−81.0	−161.7

^a See Figure 1 for atom numbering. Distances (*r*) are in pm, angles (∠) and dihedral angles (ϕ) are in degrees. Values in parentheses are the uncertainties quoted as 1σ values.

Gas electron diffraction

Refinements of the experimental GED data for each of **1** and **2** were performed on the basis of models describing the molecular geometries for the three most abundant conformers. On the basis of the calculations at the B3LYP-GD3 level employing 6-311G(2d,p) basis sets on all atoms, models were written assuming C_2 point-group symmetry for each conformer. Full descriptions of the models are given in ESI and atomic coordinates for all three conformers can be found in Tables S4 and S5. The models for **1** and **2** were written with 31 and 32 parameters, respectively, and described the major conformer for each of **1** and **2**, using a series of geometric parameters that are listed in Tables S8 and S9. Slight differences in bond lengths and bond angles both within those conformers, and also between the major and minor conformers, were introduced using fixed (non-refinable) differences. For each molecule parameters p_1 – p_4 are distances, while parameters p_5 – p_{20} are angles. Different numbers of dihedral angles are required to describe **1** and **2**, with p_{21} – p_{31} and p_{21} – p_{32} being used, respectively, to rotate the trimethylsilyl groups, the methyl groups, and one $\text{SiR}(\text{SiMe}_3)_2$ [$\text{R} = \text{H}$ (**1**), CH_3 (**2**)] group with respect to the other.

During the refinements of the experimental data, restraints were applied to parameters that are poorly defined from the GED data alone using the SARACEN method.^{31–33} The restraint values for the SARACEN method are based on the B3LYP-GD3/6-311G(2d,p) optimised geometries, while the uncertainties in these values are estimated from the range of values produced from the series of geometry optimisations at different levels of theory and with different basis sets. Whilst refining the experimental data, 29 and 27 parameters were restrained, for **1** and **2**, respectively. The vibrational effects on bonded and non-bonded distances were taken into account in the form of corrections obtained from the program SHRINK³⁴ using calculated force constants. SHRINK also gave starting values for the amplitudes of vibration associated with every pair of atoms.

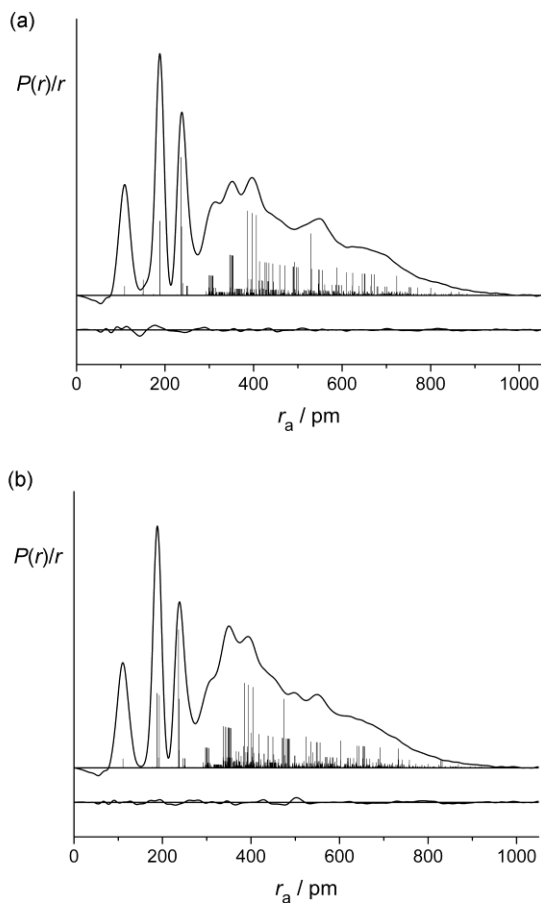
In order to refine the amplitudes of vibrations, an atom pair with the most significant scattering effect was selected for each individual peak in the radial distribution curves. All other atom pairs, with the exception non-bonded pairs including hydrogen as these contribute so little to the overall scattering, were tied using a calculated ratio to the selected pair, for which the amplitude of vibration was then refined. For both **1** and **2** eleven

amplitudes of vibration were refined, with seven restraints applied in each case. See Tables S10 and S11 for full lists of amplitudes of vibration and curvilinear distance corrections.

As mentioned earlier, only the three most abundant conformers were modelled for each of **1** and **2**. The relative amounts were recalculated to allow for only three conformers (see Tables S8 and S9 for values) and were fixed during the initial refinements. Finally, after all other parameters and amplitudes of vibration were refining, the amounts of conformers **a** and **b** were adjusted in a stepwise manner to values either side of the calculated values assumed during the initial refinement. The amount of conformer **a** was first increased in intervals of 0.05 from the initial value and then decreased from the same point, with the R_G value recorded at each step. The refinement code does not allow the amounts of conformers to be refined as part of the least-squares analysis, and so manual adjustment is the best indication we can get for the experimental amounts of the conformers. As conformer **c** was calculated by both methods to be present in much smaller abundance than **a** and **b** its value was kept constant. The compositions of **1** and **2** that yielded the lowest R factors were close to those compositions calculated using B3LYP-GD3/6-311G(2d,p). Figure S1 shows plots of the amounts of conformers **1a** and **2a** against $R_G/R_G(\text{min.})$, with these theoretical values falling within the 95% confidence limit as indicated in Figure S1.³⁵ The final R factors are based on amounts equal to amounts 0.592 of **1a**, 0.300 of **1b**, and 0.108 of **1c** being modelled, and 0.411 of **2a**, 0.450 of **2b**, and 0.139 of **2c**. From Figure S1 we estimate the uncertainty on the abundance of conformers **a** and **b** to be ± 0.100 for **1** and ± 0.150 for **2**.

Figure 2 shows the radial distribution curves from the GED refinements for **1** and **2**, with their associated experimental-minus-theoretical difference curves beneath. The related molecular intensity curves are shown in Figure S2. The R_G factors obtained from the least-square refinements for **1** and **2** are 0.073 and 0.090, respectively, while the R_D factors, which ignore the off-diagonal elements in the correlation matrix, are 0.076 and 0.053.³⁶ The experimentally-determined atomic coordinates for the three conformers of each species can be found in Tables S12 and S13.

Figure 2 Radial distribution curves and difference (theoretical-minus-experimental) curves for (a) **1**, and (b) **2**.



Discussion

For both **1** and **2** theoretical calculations (Tables 2 and 4) predict four distinct conformers with a mixture of *anticlinal*, *synclinal*, and *antiperiplanar* conformers. When comparing **1** with **2** it is interesting to note that the relative energies (shown in Tables 1 and 3) for apparently similar structures are quite different, with two different *anticlinal* conformers being low in energy for **1**, while an *anticlinal* conformer is highest in energy for **2**. One explanation for this relatively high energy in **2** is the increase in steric crowding around Si(1) and Si(2) due to the presence of methyl groups rather than hydrogen atoms (as was the case for **1**). Previous studies have been performed for 1,1,2,2-tetra-*tert*-butyl-disilane¹² (**3**), which is similar to **1** but with *tert*-butyl groups in place of trimethylsilyl groups. **3** was found to exist in a single conformation, namely an *anticlinal* arrangement with GED

determining an HSiSiH dihedral angle of $-99.4(23)^\circ$. While **1** contains two *anticlinal* configurations (**1a** and **1b**), the HSiSiH dihedral angle for **3** is closer to that of **1b** than the more abundant **1a**. The molecule **3** also has C_2 symmetry and, when viewed along the central Si–Si bond, it is apparent that one *tert*-butyl group almost eclipses another *tert*-butyl group, while the other *tert*-butyl almost eclipses a hydrogen atom.

The report on the study of **3**¹² comments on the large angle range available to silicon, with an SiSiC angle for a particular *tert*-butyl group (one that is approximately eclipsing another *tert*-butyl group) determined by GED to be $117.0(5)^\circ$, while the SiSiC angle for another *tert*-butyl group (this time one that is approximately eclipsing a hydrogen atom) reportedly much narrower at $110.7(6)^\circ$. It is useful to compare the structure of **3** with those of the *anticlinal* conformers **1a** and **1b** (Table 2). When looking down the central Si–Si bond we can see that both of these conformers are severely distorted, with certain trimethylsilyl groups almost eclipsing the hydrogen atoms, while the remaining trimethylsilyl groups on each branch are almost staggered. We find that the GED results indicate a similar range of SiSiSi angles (110.6 – 117.1°) for **1a**, and a larger range of 107.4 – 121.1° for **1b**. Conformer **1c** exists in a typical staggered arrangement with a range of SiSiSi angles of 111.6 – 118.1° . This range of angles is larger than is predicted by the computational results at a B3LYP/6-311G(2d,p) level of theory (Table 2). While the computational methods and GED results generally show good agreement for **1**, the SiSiSi angles are consistently underestimated by the computational methods; similarly there is some discrepancy between the GED and B3LYP/6-311G(2d,p) calculated values for Si–Si distances. The inclusion of dispersion effects [B3LYP-GD3/6-311G(2d,p)] improves the agreement between the calculated Si–Si bond lengths and those from the GED study, although the SiSiSi angle discrepancy remains. These effects are almost certainly because the basis sets used here do not approach the basis set limit; larger basis sets for molecules of this size are prohibitively expensive for this study.

For conformers **1a**–**1c**, the Si(5)Si(1)Si(6) angles between the two symmetrically unique trimethylsilyl groups vary by several degrees, with conformer **1c** having the narrowest angle at 111.6° , while conformer **1a** has the widest angle at 113.5° . This narrower angle in conformer **1c** results in the methyl groups on adjacent branches being closer together than in the other conformers resulting in more H···H interactions.

Comparison of the structures of **1** and **3** suggests that the most important parameter in determining the structure of **3** is the C–C distance from the tertiary carbon atom to the methyl groups' carbon atoms. While the ranges of SiSiC angles in **1** and equivalent SiCC angles in **3** are similar, the longer Si–C bond limits the degree of steric crowding in **1** and comparatively lessens the H···H interactions between the ends of the molecule. This allows the angle range around silicon to be greater and the central Si–Si bond in **1** can be considerably shorter at around 237 pm, compared to 245 pm for **3**. It is perhaps these reasons that explain why **1** can exist in multiple conformations, while **3** displays only a single conformation.

When the additional methyl groups are positioned on Si(1) and Si(2), as is the case for **2**, some interesting structural effects are observed (Table 4). The SiSiSi angles from the central Si–Si bond out to the branches shows a much smaller range for **2** than for **1**, with Si(2)Si(1)Si(5) and Si(2)Si(1)Si(6) both varying only by approximately 3° across all conformers. A widening of the Si(1)Si(5)C(31) and Si(1)Si(6)C(51) angles is also observed.

The most abundant conformer (**2a**) has a number of notable structural features that contribute to its low energy. The groups at each end of the molecule are almost perfectly staggered. Both the angles from the central silicon atoms to the trimethylsilyl groups are wider than for conformer **2b**, while one is wider and the other comparable to those in **2c**, and the Si(2)Si(1)C(55) angle is the narrowest observed for any of the conformers. These features result in the methyl groups being pushed closer together, creating more space for the bulky trimethylsilyl groups.

We note that the Si(1)–C_{Me} distance, at 193.3(19) pm, is approximately 5 pm longer than that in the relatively unstrained molecule Si₂Me₆, where an Si–C distance of 187.7(3) pm,⁶ is observed by GED. It seems that for **2** the bulky substituents push this methyl group further away from the silicon backbone. The Si–C distances in the trimethylsilyl groups are approximately 5 pm shorter than the central Si–C distance and hence are in better agreement with the value observed in Si₂Me₆.

For comparison, calculations were also performed for the hyper-substituted hexakis(trimethylsilyl)disilane (**4**) at the B3LYP/6-311G(2d,p) level. These calculations indicate that this molecule has *S*₆ point-group symmetry, with calculations performed

assuming C_{3h} symmetry determining that this was not a potential-energy minimum. By comparing the structures calculated at B3LYP/6-311G(2d,p) with the calculations of **1** and **2** at the same level of theory we find that there is a lengthening of all the SiSi bonds with the central SiSi bond measuring 247.1 pm, approximately 7 pm longer than in **1** and 8 pm longer than in **2**. The Si–SiMe₃ distances for **4** are approximately 4 and 3 pm longer than for **1** and **2**, respectively. While the angles between the central Si atoms and the branches remain within the same range observed for the conformers of both **1** and **2**, the angle between adjacent branches has reduced significantly to 103.5°. Whereas for **1** and **2** the presence of the smaller R groups provided more space for the larger SiMe₃ groups allowing the molecule to distort, the inclusion of a third SiMe₃ onto each branch means that the molecule remains in only one conformation (the staggered S_6 structure) as this allows the maximum space between the bulky SiMe₃ groups.

Previously, hexa-*tert*-butyl-disilane (**5**) has been studied and shown to be similar in structure to **4** but with *tert*-butyl groups in place of trimethylsilyl groups. Determining the structure of this molecule using GED was not possible because it dissociated into radicals.¹⁵ Calculations, however, were performed and it is useful to compare these with the calculations for the structure of **4**. The results show similar trends to those observed when comparing the structures of **1** and **3**, the shorter C–C and Si–C bond lengths in **5** compared to the Si–C and Si–Si in **4** mean that angle between the central silicon atoms and the branches are wider in the trimethylsilyl species than in the *tert*-butyl species, again allowing **4** to have a significantly shorter central Si–Si bond length of 247.1 pm (compared to 272.1 pm in **5**).

These bulky silicon-containing systems continue to provide a rich source of structural chemistry with interesting features. Subtle structural differences are observed between Si₂(SiMe₃)₄R₂ (R = H, Me), with the range of angles about the central silicon atoms and adopted conformations intimately related to the nature of the R substituent. The Si–R bond lengths are elongated compared to the parent Si₂H₆ and Si₂Me₆ systems, indicating steric effects. There are also subtle differences observed when Si₂Bu^{*t*}₄H₂ and Si₂(SiMe₃)₄H₂ are compared, with the slightly longer Si–SiMe₃ bonds compared to Si–CMe₃ bonds enabling far more conformational flexibility and a reduction in the range of angles about the central silicon atoms. The final system in this series to be studied is by GED is the hyper-

substituted $\text{Si}_2(\text{SiMe}_3)_6$ (**4**), which will be reported in the near future. It is anticipated that, on the basis of the calculated results presented in this work, the longer Si–SiMe₃ bonds will mean that the molecule will not dissociate, unlike the *tert*-butyl analogue, which dissociated into radicals.

Acknowledgements

J.S. thanks ERASMUS for funding a summer internship at the University of Edinburgh. We are grateful to the EPSRC for funding the electron diffraction research and a Fellowship for D.A.W. (EP/C513649 and EP/I004122). S.L.M. thanks the Royal Society of Edinburgh for a BP/RSE Personal Research Fellowship, and the Royal Society of Chemistry for the award of a JWT Jones Travelling Fellowship, which funded the research trip to Graz. We acknowledge the use of the EPSRC UK National Service for Computational Chemistry Software (NSCCS) hosted at Imperial College in carrying out this work, which also made use of the resources provided by the Edinburgh Compute and Data Facility (<http://www.ecdf.ed.ac.uk/>), which is partially supported by the eDIKT initiative (<http://www.edikt.org.uk>).

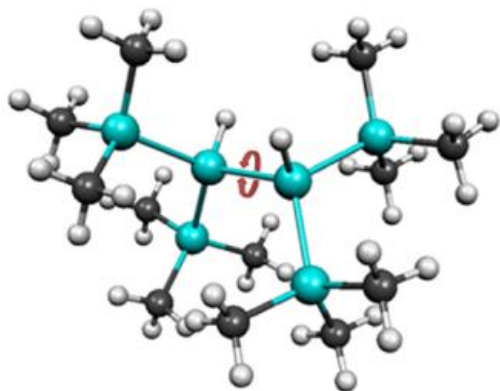
References

1. A. Bauer, T. Kammel, B. Pachaly, O. Schäfer, W. Schindler, V. Stanjek and J. Weis, *Organosilicon Chemistry V* (Eds.: N. Auner and J. Weis), Wiley-VCH, Weinheim, 2003, 527
2. a) S. Yao, *D.Phil. Thesis*, Johannes-Gutenberg-Universität Mainz, 2005; b) K. W. Klinkhammer and W. Schwarz, *Angew. Chem. Int. Ed.*, 1995, **34**, 12.
3. B. Beagley, A. R. Conrad, J. M. Freeman, J. J. Monaghan, B. G. Norton and G. C. Holywell, *J. Mol. Struct.*, 1972, **11**, 371.
4. D. W. H. Rankin and H. E. Robertson, *J. Mol. Struct.*, 1975, **27**, 438.
5. Y. Morino and E. Hirota, *J. Chem. Phys.*, 1958, **28**, 185.
6. B. Beagley, J. J. Monaghan and T. G. Hewitt, *J. Mol. Struct.*, 1971, **8**, 401.
7. H. Thomassen, K. Hagen, R. Stølevik and K. Hassler, *J. Mol. Struct.*, 1986, **147**, 331.
8. E. Røhmen, K. Hagen, R. Stølevik, M. Pöschl and K. Hassler, *J. Mol. Struct.*, 1991, **244**, 41.

9. D. Hnyk, R. S. Fender, H. E. Robertson, D. W. H. Rankin, M. Bühl, K. Hassler and K. Schenzel, *J. Mol. Struct.*, 1995, **346**, 215.
10. B. A. Smart, H. E. Robertson, N. W. Mitzel, D. W. H. Rankin, R. Zink and K. Hassler, *J. Chem. Soc., Dalton Trans.*, 1997, 2475.
11. S. L. Hinchley, B. A. Smart, C. A. Morrison, H. E. Robertson, D. W. H. Rankin, R. Zink and K. Hassler, *J. Chem. Soc., Dalton Trans.*, 1999, 2303.
12. S. L. Hinchley, H. E. Robertson, A. Parkin, D. W. H. Rankin, G. Tekautz and K. Hassler, *Dalton Trans.*, 2004, 759.
13. B. Albisson, H. Teramae, J. W. Downing and J. Michl, *Chem. Eur. J.*, 1996, **2**, 529.
14. a) N. Wilberg, H. Schuster, A. Simon and K. Peters, *Angew. Chem.*, 1986, **98**, 100; b) N. Wilberg, H. Schuster, A. Simon and K. Peters, *Angew. Chem. Int. Ed. Engl.*, 1986, **25**, 79.
15. S. L. Masters, D. A. Grassie, H. E. Robertson, M. Höbling and K. Hassler, *Chem. Commun.*, 2007, 2618.
16. U. Baumeister, K. Schenzel, R. Zink and K. Hassler, *J. Organometal. Chem.*, 1997, **543**, 117.
17. G. Kollegger and K. Hassler, *J. Organometal. Chem.*, 1995, **485**, 233.
18. M. J. Frisch, G. W. Trucks, H. B. Schlegel, G. E. Scuseria, M. A. Robb, J. R. Cheeseman, G. Scalmani, V. Barone, B. Mennucci, G. A. Petersson, H. Nakatsuji, M. Caricato, X. Li, H. P. Hratchian, A. F. Izmaylov, J. Bloino, G. Zheng, J. L. Sonnenberg, M. Hada, M. Ehara, K. Toyota, R. Fukuda, J. Hasegawa, M. Ishida, T. Nakajima, Y. Honda, O. Kitao, H. Nakai, T. Vreven, J. A. Montgomery, Jr., J. E. Peralta, F. Ogliaro, M. Bearpark, J. J. Heyd, E. Brothers, K. N. Kudin, V. N. Staroverov, T. Keith, R. Kobayashi, J. Normand, K. Raghavachari, A. Rendell, J. C. Burant, S. S. Iyengar, J. Tomasi, M. Cossi, N. Rega, J. M. Millam, M. Klene, J. E. Knox, J. B. Cross, V. Bakken, C. Adamo, J. Jaramillo, R. Gomperts, R. E. Stratmann, O. Yazyev, A. J. Austin, R. Cammi, C. Pomelli, J. W. Ochterski, R. L. Martin, K. Morokuma, V. G. Zakrzewski, G. A. Voth, P. Salvador, J. J. Dannenberg, S. Dapprich, A. D. Daniels, Ö. Farkas, J. B. Foresman, J. V. Ortiz, J. Cioslowski, D. J. Fox, Gaussian 09, Revision D.01, Gaussian, Inc., Wallingford CT, 2013.
19. Edinburgh Compute and Data Facility (ECDF); <http://www.ecdf.ed.ac.uk/>.

20. EPSRC-funded National Service for Computational Chemistry Software (NSCCS); <http://www.nscs.ac.uk/>.
21. A. Becke, *J. Chem. Phys.*, 1993, **98**, 5648.
22. C. Lee, W. Yang and R. Parr, *Phys. Rev. B*, 1988, **37**, 785.
23. B. Miehlich, A. Savin, H. Stoll and H. Preuss, *Chem. Phys. Lett.*, 1989, **157**, 200.
24. J. Binkley, J. A. Pople and W. J. Hehre, *J. Am. Chem. Soc.*, 1980, **102**, 939.
25. M. Gordon, J. Binkley, J. A. Pople, W. J. Pietro and W. J. Hehre, *J. Am. Chem. Soc.*, 1982, **104**, 2797.
26. S. Grimme, J. Antony, S. Ehrlich and H. Krieg, *J. Chem. Phys.*, 2010, **132**, 154104.
27. C. M. Huntley, G. S. Laurensen and D. W. H. Rankin, *J. Chem. Soc., Dalton Trans.*, 1980, 954.
28. H. Fleischer, D. A. Wann, S. L. Hinchley, K. R. Borisenko, J. R. Lewis, R. J. Mawhorter, H. E. Robertson and D. W. H. Rankin, *Dalton Trans.*, 2004, 3221.
29. S. L. Hinchley, H. E. Robertson, K. R. Borisenko, A. R. Turner, B. F. Johnston, D. W. H. Rankin, M. Ahmadian, J. N. Jones and A. H. Cowley, *Dalton Trans.*, 2004, 2469.
30. A. W. Ross, M. Fink and R. Hilderbrandt, *International Tables for Crystallography*, Ed. A. J. C. Wilson, Kluwer Academic Publishers, Dordrecht, The Netherlands, **1992**, vol. C, p.245.
31. N. W. Mitzel, B. A. Smart, A. J. Blake, H. E. Robertson and D. W. H. Rankin, *J. Phys. Chem.*, 1996, **100**, 9339.
32. A. J. Blake, P. T. Brain, H. McNab, J. Miller, C. A. Morrison, S. Parsons, D. W. H. Rankin, H. E. Robertson and B. A. Smart, *J. Phys. Chem.*, 1996, **100**, 12280.
33. N. W. Mitzel and D. W. H. Rankin, *Dalton Trans.*, 2003, 3650.
34. V. A. Sipachev, *J. Mol. Struct. (THEOCHEM)*, 1985, **121**, 143.
35. W. C. Hamilton, *Acta Cryst.*, 1965, **18**, 502.
36. S. L. Masters, S. J. Atkinson, M. Höbbling and K. Hassler, *Struct. Chem.*, 2013, **24**, 1201.

Graphical Abstract



The structures of 1,1,2,2-tetrakis(trimethylsilyl)disilane and 1,1,2,2-tetrakis(trimethylsilyl)-dimethyldisilane have been determined by gas electron diffraction. The presence of bulky and flexible trimethylsilyl groups dictates many aspects of the geometric structures in the gas phase, with the molecules adopting structures to reduce steric strain.